526

VOLUME 80 SEPARATE No. 526

PROCEEDINGS

AMERICAN SOCIETY
OF
CIVIL ENGINEERS

OCTOBER, 1954

VERIFICATION OF THEORY FOR OBLIQUE STANDING WAVES

by Arthur T. Ippen, M. ASCE, and
Donald R. F. Harleman, J.M. ASCE

ENGINEERING MECHANICS
DIVISION

{Discussion open until February 1, 1955}

Copyright 1954 by the AMERICAN SOCIETY OF CIVIL ENGINEERS
Printed in the United States of America

Headquarters of the Society
33 W. 39th St.
New York 18, N. Y.

PRICE $0.50 PER COPY

THIS PAPER

--represents an effort by the Society to deliver technical data direct from the author to the reader with the greatest possible speed. To this end, it has had none of the usual editing required in more formal publication procedures.

Readers are invited to submit discussion applying to current papers. For this paper the final date on which a discussion should reach the Manager of Technical Publications appears on the front cover.

Those who are planning papers or discussions for "Proceedings" will expedite Division and Committee action measurably by first studying "Publication Procedure for Technical Papers" (Proceedings – Separate No. 290). For free copies of this Separate—describing style, content, and format—address the Manager, Technical Publications, ASCE.

Reprints from this publication may be made on condition that the full title of paper, name of author, page reference (or paper number), and date of publication by the Society are given.

The Society is not responsible for any statement made or opinion expressed in its publications.

This paper was published at 1745 S. State Street, Ann Arbor, Mich., by the American Society of Civil Engineers. Editorial and General Offices are at 33 West Thirty-ninth Street, New York 18, N. Y.

VERIFICATION OF THEORY FOR OBLIQUE STANDING WAVES

Arthur T. Ippen,[1] M. ASCE
and Donald R. F. Harleman,[2] J. M. ASCE

SYNOPSIS

Changes in section or alignment of open channels flowing at supercritical velocities give rise to depth changes which may be abrupt or gradual depending on the type of wave produced. A series of experiments were undertaken to verify the hydrodynamic theory for both oblique hydraulic jumps and expansion waves with Froude numbers ranging from two to seven. The position of the standing waves caused by a wall deflection and the associated depth changes were observed and compared with existing theory. The average agreement was of the order of two per cent for oblique jumps with a somewhat larger discrepancy for the expansions depending on the magnitude of the wall deflection.

An analysis and experimental observations of the nature of the transition between undular and roller type jumps is presented. It is shown that the transition occurs at a depth ratio of two.

INTRODUCTION

The publication in 1949 of the Symposium on High Velocity Flow in Open Channels[3] made available to the engineering profession a unified treatment and general method of design for supercritical flow in hydraulic structures. Since that time, experimental information relating to oblique standing waves has been obtained in the Hydrodynamics Laboratory of the Massachusetts Institute of Technology. The experiments have served to verify much of the basic theory underlying the mechanics of supercritical flow as used for example in the design of channel and spillway transitions and their results are presented to further the broad acceptance of the principles involved. Such acceptance is rightly dependent upon adequate experimental confirmation of the basic theory. In addition, the experiments revealed some interesting correlations between oblique jumps and the general theory of irrotational translation waves.

---

1. Prof. of Hydraulics, Massachusetts Inst. of Technology, Cambridge, Mass.
2. Asst. Prof. of Hydraulics, Massachusetts Inst. of Technology, Cambridge, Mass.
3. "High Velocity Flow in Open Channels," A Symposium by A. T. Ippen, R. T. Knapp, J. H. Dawson, H. Rouse, B. V. Bhoota and E. Y. Hsu, Trans. ASCE, Vol. 116, 1951, p. 265.

The experimental work is divided into two phases, the first of which deals with the oblique hydraulic jump (also called the oblique shock wave by analogy to the supersonic case). This type of jump is produced when a vertical boundary is deflected inward to the flow as in the case of a channel contraction. This condition results in an abrupt increase along a jump front which is propagated from the point of boundary discontinuity and depends in magnitude on the angle of deflection. The limiting case of the oblique standing wave is the familiar hydraulic jump in which the front is normal to the direction of flow.

The second phase deals with the opposite situation of an expansion wave produced when a vertical boundary is deflected outward from the supercritical flow as in a channel expansion. Since a negative hydraulic jump is physically impossible, this boundary condition must result in a gradual decrease in the depth of the flow defined by lines of constant depth radiating from the boundary discontinuity. The extreme case of an expansion wave is represented by the abrupt termination of the side walls with the channel bottom continuing at the same slope. This case has been investigated experimentally by Rouse, Bhoota and Hsu.[3]

All of the waves investigated were of the standing wave type, that is, the wave fronts were stationary and the flow was steady.

Theoretical Background

The derivation of the foundamental relationships for both the oblique jump and expansion waves are presented in detail in the symposium cited; therefore, only a summary of the theory is included in this paper. In addition, however, a more detailed analytical investigation for the transition from the undular to the roller type jump is presented which has not been treated so far.

Oblique Hydraulic Jump

For purposes of definition, Fig. 1a shows the conditions which are to be investigated. If a boundary wall is deflected into a supercritical stream through an angle θ, an oblique hydraulic jump will occur as a standing wave at an angle β with respect to the original flow direction. The velocities and depths before and after the jump are designated V_1, V_2 and h_1, h_2, respectively, as shown in Fig. 1a. Velocity components normal to the wave front are V_{n1} and V_{n2}. This analysis is concerned only with initial and final conditions of flow which are independent of the character of the depth change taking place across the jump.

Application of the steady flow continuity and momentum relationships in the direction normal to the wave front together with an equation obtained from the geometry of the velocity vector diagram provides a total of three independent equations.

$$\text{Continuity:} \quad h_1 V_{n1} = h_2 V_{n2} \tag{1}$$

$$\text{Momentum:} \quad \frac{g}{2}(h_2^2 - h_1^2) = h_1 V_{n1}(V_{n1} - V_{n2}) \tag{2}$$

Geometry (Fig. 1a): $\frac{\tan \beta}{\tan (\beta - \theta)} = \frac{V_{n1}}{V_{n2}}$ (3)

(Since $V_{t1} = V_{t2}$)

Solving Eq. (2) for V_{n1} and eliminating V_{n2} by Eq. (1), the familiar hydraulic jump relation is obtained:

$$V_{n1} = \sqrt{gh_1} \sqrt{\frac{1}{2} \frac{h_2}{h_1} \left(1 + \frac{h_2}{h_1}\right)} \tag{4a}$$

and the Froude number normal to the jump front is thus

$$F_{n1} = \sqrt{\frac{1}{2} \frac{h_2}{h_1} \left(1 + \frac{h_2}{h_1}\right)} \tag{4b}$$

Since the actual flow velocity $V_1 = \frac{V_{n1}}{\sin \beta}$ and the initial Froude number $F_1 = \frac{V_1}{\sqrt{gh_1}}$, the above equation can also be written as:

$$\sin \beta = \frac{1}{F_1} \sqrt{\frac{1}{2} \left(\frac{h_2}{h_1}\right) \left(1 + \frac{h_2}{h_1}\right)} \tag{4c}$$

The characteristics of the oblique hydraulic jump are completely determined if any three independent variables of the six quantities, h_1, h_2, F_1, F_2, β and θ, are specified. In the practical application of oblique jump theory, it is usually convenient to consider the initial Froude number F_1, the initial depth h_1 and the boundary deflection angle θ as the independent variables. With these known quantities, the wave angle β and the depth ratio $\frac{h_2}{h_1}$ may be determined.

Eq. (4c) when solved for the depth ratio becomes:

$$\frac{h_2}{h_1} = \frac{1}{2} \left(\sqrt{1 + 8F_1^2 \sin^2 \beta} - 1\right) \tag{5}$$

Eqs. (1) and (3) can be combined to yield,

$$\frac{h_2}{h_1} = \frac{\tan \beta}{\tan (\beta - \theta)} \tag{6}$$

If Eqs. (5) and (6) are equated, a relation involving F_1, θ and β is obtained,

$$\tan\theta = \frac{\tan\beta\left(\sqrt{1 + 8F_1^2\sin^2\beta} - 3\right)}{2\tan^2\beta + \sqrt{1 + 8F_1^2\sin^2\beta} - 1} \qquad (7)$$

Inasmuch as Eq. (7) cannot be solved for β in terms of F_1 and θ, a plot of this equation is necessary for the solution of oblique jump problems. A comprehensive representation of all characteristics expressed by Eqs. (5) - (7) is given in a four-quadrant graph (see Fig. 8 of Ref. 3). The primary aim of the first phase of this investigation was the verification of Eqs. (5) and (7) over a wide range of Froude numbers and deflection angles.

Limiting Conditions for the Undular Jump

During the course of the experimental work on the oblique jump, it was observed that if the depth ratio was less than two, the jump was composed of a series of undulations while for larger depth ratio the characteristic "roller" was present. This fact has already been established by Bakhmeteff[4], [5] in his early work on the special case of the normal hydraulic jump and has since been observed by other investigators. Since the experimental determination of the angle of the oblique jump, β, is one of the objects of this study, an analytical correlation of these two forms of the jump is necessary for the interpretation of the experimental data.

The propagation velocity, c, of a constant discharge translation wave of appreciable height and curvature moving in still, shallow water is, according to Boussinesq, (see Keulegan[6])

$$c = \sqrt{gh_1}\left(1 + \frac{3}{4}\frac{y}{h_1} + \frac{h_1^2}{6y}\frac{\partial^2 y}{\partial x^2}\right) \qquad (8)$$

with the notation as shown in Fig. 2. This constant discharge translation wave can be reduced to an oblique standing wave by superimposing any steady flow having an initial stream velocity V_1 with a component V_{n1} equal and opposite to c. This implies that the tangential components V_{t1} and V_{t2} of the velocity V_1 are equal since no momentum change takes place parallel to the wave front. Eq. (8) may then be written in terms of the ratio $\frac{V_{n1}}{\sqrt{gh_1}} = F_{n1}$ which is the initial Froude number normal to the wave front.

$$F_{n1} = 1 + \frac{3}{4}\frac{y}{h_1} + \frac{h_1^2}{6y}\frac{\partial^2 y}{\partial x^2} \qquad (9)$$

4. "Hydraulics of Open Channels," by B. A. Bakhmeteff, Engineering Societies Monograph, McGraw-Hill, 1932.
5. "The Hydraulic Jump in Terms of Dynamic Similarity," by B. A. Bakhmeteff and A. E. Matzke, Trans. ASCE, Vol. 101, 1936, p. 630.
6. "Wave Motion" (Chapter XI) by G. H. Keulegan, Engineering Hydraulics, John Wiley and Sons, 1950, p. 719.

The fact that Eq. (9) is the appropriate relation for the undular hydraulic jump may be seen from the following observations:

a) The undular jump is composed of a series of oscillations of decreasing amplitude about the equilibrium depth y_2. Since Since $\frac{\partial^2 y}{\partial x^2} = 0$ when $y = y_2$, Eq. (9) becomes

$$F_{n1} = 1 + \frac{3}{4}\frac{y_2}{h_1} \qquad (9a)$$

or since $y_2 = h_2 - h_1$

$$F_{n1} = \frac{1}{4}\left(1 + 3\frac{h_2}{h_1}\right) \qquad (9b)$$

If Eq. (9b) is compared to the momentum analysis given by Eq. (4b), the results agree within 1% in the range of depth ratios from 1 to 2.

b) The entire wave is stationary with respect to the oncoming flow, therefore, the celerity of every point along the wave must be the same (i.e., $1 + \frac{3}{4}\frac{y}{h_1} + \frac{h_1^2}{6y}\frac{\partial^2 y}{\partial x^2} = \text{const.}$).

Since, at the crest of the initial oscillation the curvature $\frac{\partial^2 y}{\partial x^2}$ is negative, the height y_a of the crest must be greater than y_2 to compensate for the effect of the curvature term in Eq. (9). It also follows that since $\frac{\partial^2 y}{\partial x^2} = 0$ at the points of inflection of the oscillations, these points must all occur at the same height as the equilibrium surface for depth y_2.

Keulegan[7] has shown that the undulations at the front of a positive surge are essentially conoidal waves propagated without change of form and further, that the center of gravity of these waves, which include the solitary wave as a special limiting case, is above the original free surface by an amount equal to one-third the maximum height of the wave. By equating the propagation velocity of the center of gravity of the wave to that of the wave train itself, Keulegan concludes that the height of the initial undulation y_a is three-halves the height of the layer y_2, therefore,

$$y_a = \frac{3}{2}y_2 = \frac{3}{2}(h_2 - h_1) \qquad (10)$$

Making use of the foregoing principles, the limiting conditions for the existance of an undular jump may be obtained.

With the notation of Fig. 2, $h_a = y_a + h_1$ where h_a is the height of the

7. "Mathematical Theory of Irrotational Translation Waves," by G. H. Keulegan and G. W. Patterson, Journal of Research of the National Bureau of Standards, RP1273, Vol. 24, 1940.

initial crest above the channel bottom, eliminating y_a by means of Eq. (10),

$$h_a = \frac{3}{2} h_2 - \frac{1}{2} h_1 \qquad (11)$$

It is apparent that the total height h_a of the first undulation plus the kinetic energy head at the crest cannot exceed the energy level of the flow immediately in front of the jump. In fact, h_a, will be a maximum when it is equal to the initial energy head. At this condition, the particle velocity at the crest must be zero and thus the crest is presumed to be inherently unstable. At this point, the front will change from the undulating to the "roller" type front.

The initial energy head referred to the channel bottom is given by H_1, where

$$H_1 = h_1 + \frac{V_1^2}{2g} = h_1 + \frac{V_{n1}^2}{2g} + \frac{V_{t1}^2}{2g} \qquad (12)$$

However, the initial energy head in the flow field containing the oblique standing wave can change only with changes in $\frac{V_n^2}{2g}$ and the depth since $\frac{V_t^2}{2g}$ is a constant throughout the flow. Thus, H_{n1} alone represents the portion of the total energy head H_1 which is of significance with respect to the limiting properties of the wave front.

Therefore,

$$H_{n1} = H_1 - \frac{V_t^2}{2g} = h_1 + \frac{V_{n1}^2}{2g} \qquad (13)$$

If Eq. (11) is divided by Eq. (13), the ratio of the height of the first crest to the initial energy level is obtained,

$$\frac{h_a}{H_{n1}} = \frac{\frac{3}{2}\frac{h_2}{h_1} - \frac{1}{2}}{1 + \frac{F_{n1}^2}{2}}$$

F_{n1} can be eliminated in terms of the depth ratio $\frac{h_2}{h_1}$ across the jump by the momentum equation (4b), therefore,

$$\frac{h_a}{H_{n1}} = \frac{6\frac{h_2}{h_1} - 2}{\left(\frac{h_2}{h_1}\right)^2 + \frac{h_2}{h_1} + 4} \qquad (14)$$

A plot of Eq. (14) given in Fig. 3 shows that for $\frac{h_a}{H_{n1}} = 1$, the depth ratio becomes $\frac{h_2}{h_1} = 2$. The instability of the crest postulated for $\frac{h_a}{H_{n1}} = 1$ thus is seen to occur for the depth ratios observed in experiments and practice.

Oblique Expansion Waves

As shown in Fig. 1b, an oblique expansion wave occurs when the boundary is turned outward from the flow at an angle θ_t. A gradual depth decrease occurs which is defined by a fan-shaped region of constant depth lines delineated by the angles β_1 and β_2 measured with respect to the initial and final flow directions, where

$$\beta_1 = \sin^{-1} \frac{1}{F_1} \quad \text{and} \quad \beta_2 = \sin^{-1} \frac{1}{F_2} \tag{15}$$

F_1 and F_2 are the initial and final Froude numbers of the flow.

Assuming F_1, h_1 and θ_t are the independent variables, as in the analysis of the oblique jump, the characteristics of the expansion may be determined as follows:

The fundamental equation relating the initial and final Froude numbers to the total deflection angle θ_t is (Ref. 3)

$$\Theta_1 - \Theta = \sqrt{3} \tan^{-1} \frac{\sqrt{3}}{\sqrt{F^2 - 1}} - \tan^{-1} \frac{1}{\sqrt{F^2 - 1}} \tag{16}$$

where $\theta = 0$ when $F = F_1$
and $\theta = \theta_t$ when $F = F_2$
Thus, when F_1 and θ_t are given, F_2 is obtained from Eq. (16) or its graph (see Fig. 3 of Ref. 3) and the angular region in which the depth change takes place is found from Eq. (15). Since the depth change takes place without perceptible energy dissipation, the depth at any point in the flow is uniquely related to the magnitude of the local Froude number. Equating the specific energy heads before and after the expansion,

$$h_1 + \frac{V_1^2}{2g} = h_2 + \frac{V_2^2}{2g}$$

and dividing through by h_1 and rearranging, the expression for the total depth change is obtained.

$$\frac{h_2}{h_1} = \frac{F_1^2 + 2}{F_2^2 + 2} \tag{17}$$

The second phase of the experimental work is concerned with the verification of the foregoing equations.

Experimental Equipment and Procedure

All of the experimental investigations were conducted in the high-velocity channel in the Hydrodynamics Laboratory of M. I. T. The rectangular channel is approximately 40 feet long, 4 feet wide and one foot in depth. The floor consists of half-inch plate glass and the side walls are constructed of carefully aligned aluminum plate. The entire channel can be set to any desired slope up to 8% by the push-button operation of an electrically driven spindle lifting mechanism. The magnitude of the slope is obtained by a calibrated revolution counter attached to the spindle driving mechanism. Water from the main laboratory supply system enters the channel through a converging nozzle 4 feet wide which can be set to admit water to the test section at any depth up to 4 inches. Water depths are measured by a point gage attached to a dial indicator reading to 0.01 inches and velocities are measured by a Prandtl tube 3/16" in diameter. A Venturi meter in the supply line provides for measurement of the discharge.

The desired oblique jumps or flow expansion zones were produced by a deflector vane approximately 7 feet long and one foot high located 15 feet downstream from the nozzle. The vane was arranged so that it could be fixed in various positions up to a maximum angle of $\theta = 21^{\circ}$ in three degree increments. In the case of the oblique jumps, the hinge was placed four inches away from the channel wall so as to be independent of the side wall boundary effects. Expansion waves were produced by the same vane with the hinge set 18 inches from the channel wall. A lead vane set parallel to the channel walls was used to determine the effect of a controlled side wall boundary layer on the characteristics of the standing waves.

For a given run, values of the three independent variables F_1, h_1 and θ were chosen. The discharge and depth were chosen to give a desired nominal Froude number and the slope of the flume was adjusted to produce uniform flow. The actual values of F_1 and h_1 were then determined from Pitot tube and point gage traverses of the channel cross section with the deflector vane set at zero degrees.

Oblique Jump Experiments

In the series of experiments dealing with oblique hydraulic jumps, a total of 52 runs were made with nine initial Froude numbers ranging from a minimum of 2.00 to a maximum of 7.00 at initial depths of 0.90 and 1.50 inches. Figure 4 shows a series of three photographs of oblique standing waves looking downstream along the deflector vane. In Fig. 4a, the deflection angle is 9° and the depth ratio across the jump is 1.56, the undular form of the wave is clearly shown by comparison with Fig. 4b at $\theta = 15^{\circ}$ and a depth ratio of 2.00. In agreement with the analysis previously given, the crest has become unstable and the jump front is much more abrupt due to the presence of a roller. The final photograph shows the limiting deflecting angle (in this case $\theta = 21^{\circ}$) imposed by the finite width of the channel. This so-called "choking" condition is brought about when the reflection of the initial shock wave from the right-hand wall strikes the downstream end of the deflector vane. If the local Froude

number at this point becomes less than unity a normal hydraulic jump will gradually move upstream and come to rest near the leading edge of the deflector vane. For certain cases, it was possible to delay the formation of the normal jump by adding energy to the flow in the form of a jet of water introduced along the right-hand wall near the point at which the initial wave was reflected.

The experimental data required for the determination of the wave angle β and the corresponding depth ratio across the jump were obtained by taking depth profiles transversely across the flow starting at the deflector vane and extending to the right-hand wall of the channel. These profiles were taken at one-foot intervals downstream from the leading edge of the vane.

Expansion Zone Experiments

In the series of experiments on the characteristics of expansion zones, a total of 27 runs were made at Froude numbers of 1.95 and 2.94 for initial depths of 0.90 and 1.50 inches. The experimental procedure was the same as that used in the study of the oblique jumps.

Experimental Results

Oblique Standing Waves

For a given experimental run with F_1, h_1 and θ determined in advance, the depth ratio $\frac{h_2}{h_1}$ and wave angle β were found in the following manner:

A plot of the experimental data was made in which a plan view of the test section is represented to the same longitudinal and transverse scale. The wave profiles are then plotted at their respective longitudinal stations; the actual depths being plotted to an exaggerated vertical scale independent of the longitudinal scale. The resulting plot gives a "perspective" view of the jump front while retaining all dimensions in true scale, the only restriction being that angles be measured in the plane of the channel bottom. Two plots of this type are shown in Figs. 5 and 6 at Froude numbers of 2.08 for a 9^o deflection angle and 4.18 for a 15^o deflection angle. Figure 5 illustrates a wave form characteristic of the undular jump while Fig. 6 is typical of the roller type jump at depth ratios larger than two.

In the case of undular jumps, the depth h_2 is readily determined from the equilibrium depth and the points of inflection of the undulations as shown by the dashed line representing this depth in the profiles of Fig. 5. It has also been repeatedly observed that the height of the initial crest is $\frac{3}{2}(h_2 - h_1)$ as was previously predicted. In the case of the roller type jumps, the depth h_2 is less easily defined due to the intense surface disturbances near the front. In this case, the depth at the deflector vane is used. The final value of $\frac{h_2}{h_1}$ for each run is the average of the individual ratios for the several transverse depth profiles.

The method for the experimental determination of the wave angle β is one which applies equally well to undular or roller type jumps. The location of the wave front for a particular profile is approximately by a vertical line drawn so that the triangular areas (above and below the wave profile) formed by the horizontal depth lines h_1 and h_2 and the vertical line are equal. The intersection of this line with the channel bottom is marked for each profile and a straight line is drawn through the points to determine the angle of the standing wave with respect to the oncoming flow. This somewhat arbitrary method has the advantage of not placing undue weight upon any one measured point on the wave front; this is important in the case of the roller type jumps where depth measurements are difficult.

This line from which the wave angle is measured may not pass exactly through the point of boundary discontinuity due to the finite thickness of the wave front.

The experimental results and comparison with theory are summarized in Table I. Figure 7 shows the comparisons in graphical form. The wave angle β is plotted against the deflection angle and the depth ratio for the various initial Froude numbers For clarity, the curves are separated according to their nominal initial depths of 0.90 and 1.50 inches. The average agreement between theory and experiment for both the wave angle and the depth ratio is of the order of two per cent. Larger differences appear for the minimum and maximum deflection angles due, in the former case, to the small depth changes involved and to the eddying of the roller and large vertical accelerations in the latter case.

The depth ratio may also be presented in a much simpler manner in terms of the Froude number normal to the wave front F_{n1} which can be calculated from the experimental values of F_1 and β since $F_{n1} = F_1 \sin \beta$. The right-hand curves of Fig. 7 are then reduced to a single curve which represents the momentum equation of the normal hydraulic jump (Eq. (4b)). For each experimental run, the value of F_{n1} was calculated and plotted for the corresponding experimental depth ratio as shown in Fig. 8. In addition, a classification of "undular," or "roller" was assigned to each run by observing the form of the wave profile. In a few runs the classification was not clear and these runs were labeled "transition." It is seen from Fig. 8 that the regions of the two wave types are clearly defined and confirm the analysis which indicated the limit of undular jumps at a depth ratio of two.

Expansion Waves

The experimental depth profiles of the expansion wave were plotted in the same manner as before. A representative plot is shown in Fig. 9 for the conditions $F_1 = 2.94, \theta_t = 15^\circ$ and $h_1 = 0.90$ in. Superimposed upon the experimental depths are the theoretical water depth profiles shown as dashed lines. The characteristic or constant depth lines are also shown in increments of three degrees of expansion; thus the beginning and end of the theoretical expansion zone is determined by the initial and final line of this series radiating from the leading edge of the deflector vane. In general, both the slope and position of the experimental profile agree reasonably well with the theoretical one except for

the region close to the leading edge. In this portion, the non-hydrostatic pressure distribution due to large vertical accelerations accounts for this disagreement. In the region of constant depth h_2 between the deflector vane and the last disturbance line, the experimental value of h_2 is determined for each profile by finding the best horizontal line through the experimental points. Figure 10 gives an indication of the rapid drop of the depth near the turn-off point, showing the wall profiles along the vane for various deflection angles θ. The depth ratios for all runs are summarized as a function of total deflection angle and initial Froude number in Fig. 11. The general trend exhibited by the measured depths is toward slightly higher values of h_2 than are given by theory. This tendency is undoubtedly due to the displacement effect of the boundary layer which in this region assumes a greater percentage of the total depth since h_2 is considerably smaller than the initial depth h_1.

ACKNOWLEDGMENTS

The experimental results contained herein were obtained under Contract W33-038-ac-16703 as part of a study of the validity of the hydraulic analogy to supersonic flow sponsored by the United States Air Force, Air Materiel Command. The assistance of Mr. C. E. Carver, Jr., Research Assistant, is hereby acknowledged.

TABLE I

SUMMARY OF EXPERIMENTAL RESULTS
ON OBLIQUE STANDING WAVES

Run	Froude No.	Defl. Angle	Wave Angle	Wave Angle	Depth Ratio	Depth Ratio		Run	Froude No.	Defl. Angle	Wave Angle	Wave Angle	Depth Ratio	Depth Ratio
	F_1	θ	β Exp.	β Theor.	h_2/h_1 Exp.	h_2/h_1 Theor.			F_1	θ	β Exp.	β Theor.	h_2/h_1 Exp.	h_2/h_1 Theor.
I-1	2.00	3°	33.4	33.2	1.12	1.12		C-5	3.80	15°	29.6	29.5	2.13	2.19
I-2	2.00	6°	35.2	36.6	1.25	1.26		C-6	3.80	18°	32.6	32.7	2.38	2.45
I-3	2.00	9°	39.0	40.3	1.39	1.40		C-7	3.80	21°	36.0	36.1	2.66	2.70
I-4	2.00	12°	43.0	44.6	1.52	1.54								
								J-1	4.18	3°	15.0	16.3	1.24	1.24
D-1	2.08	3°	31.7	31.9	1.13	1.13		J-2	4.18	6°	18.5	18.9	1.48	1.49
D-2	2.08	6°	33.8	35.1	1.26	1.26		J-3	4.18	9°	21.4	21.8	1.76	1.76
D-3	2.08	9°	38.2	38.8	1.39	1.40		J-4	4.18	12°	24.2	24.8	2.06	2.03
D-4	2.08	12°	41.6	42.8	1.55	1.55		J-5	4.18	15°	27.6	27.8	2.36	2.32
								J-6	4.18	18°	30.8	31.1	2.62	2.59
B-1	3.05	3°	20.9	21.8	1.15	1.17								
B-2	3.05	6°	24.0	24.6	1.31	1.36		G-1	5.91	3°	12.4	12.2	1.26	1.34
B-3	3.05	9°	27.0	27.6	1.52	1.56		G-2	5.91	6°	14.5	15.0	1.61	1.70
B-4	3.05	12°	29.4	30.6	1.70	1.76		G-3	5.91	9°	17.4	17.6	2.02	2.10
B-5	3.05	15°	33.2	34.0	1.93	1.96		G-4	5.91	12°	20.2	20.6	2.41	2.49
B-6	3.05	18°	36.6	37.4	2.11	2.17		G-5	5.91	15°	23.1	23.6	2.94	2.90
								G-6	5.91	18°	25.6	26.7	3.33	3.29
F-1	3.20	3°	21.8	20.8	1.18	1.18								
F-2	3.20	6°	23.4	23.6	1.37	1.38		H-1	6.30	3°	11.6	11.6	1.35	1.36
F-3	3.20	9°	26.2	26.5	1.56	1.58		H-2	6.30	6°	14.1	14.2	1.74	1.75
F-4	3.20	12°	29.0	29.6	1.78	1.79		H-3	6.30	9°	17.2	17.1	2.14	2.16
F-5	3.20	15°	32.4	32.8	2.00	2.00		H-4	6.30	12°	19.6	20.0	2.58	2.59
F-6	3.20	18°	35.6	36.2	2.24	2.22								
F-7	3.20	21°	39.0	39.8	2.45	2.44		E-1	7.00	3°	10.3	10.6	1.44	1.41
								E-2	7.00	6°	12.9	13.4	1.87	1.83
C-1	3.80	3°	17.4	17.8	1.2	1.22		E-3	7.00	9°	15.7	16.2	2.26	2.30
C-2	3.80	6°	19.8	20.4	1.43	1.45		E-4	7.00	12°	18.4	19.1	2.67	2.78
C-3	3.80	9°	23.1	23.3	1.66	1.69		E-5	7.00	15°	20.3	22.1	3.32	3.26
C-4	3.80	12°	26.4	26.4	1.89	1.94		E-6	7.00	18°	23.6	25.2	4.00	3.72

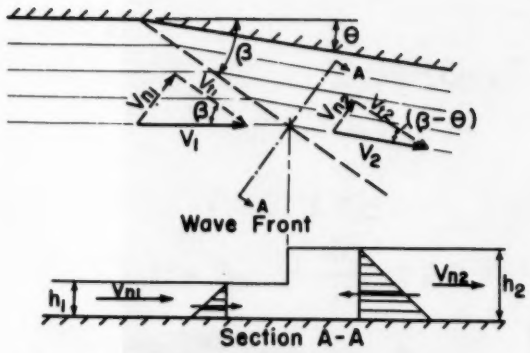

Fig. 1a. Oblique Hydraulic Jump

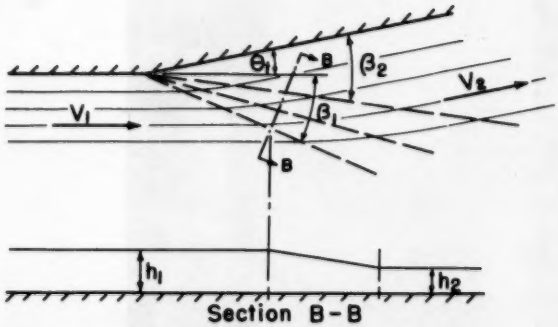

Fig. 1b. Oblique Expansion Wave

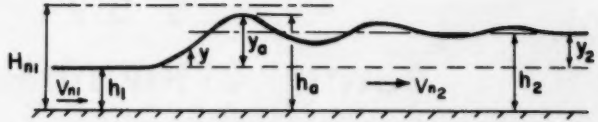

Profile of Typical Undular Jump

Fig. 2

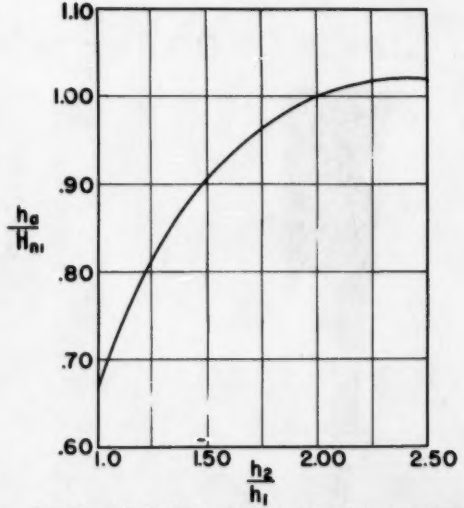

Ratio of Initial Crest Height to Total Energy vs. Depth Ratio of Jump

Fig. 3

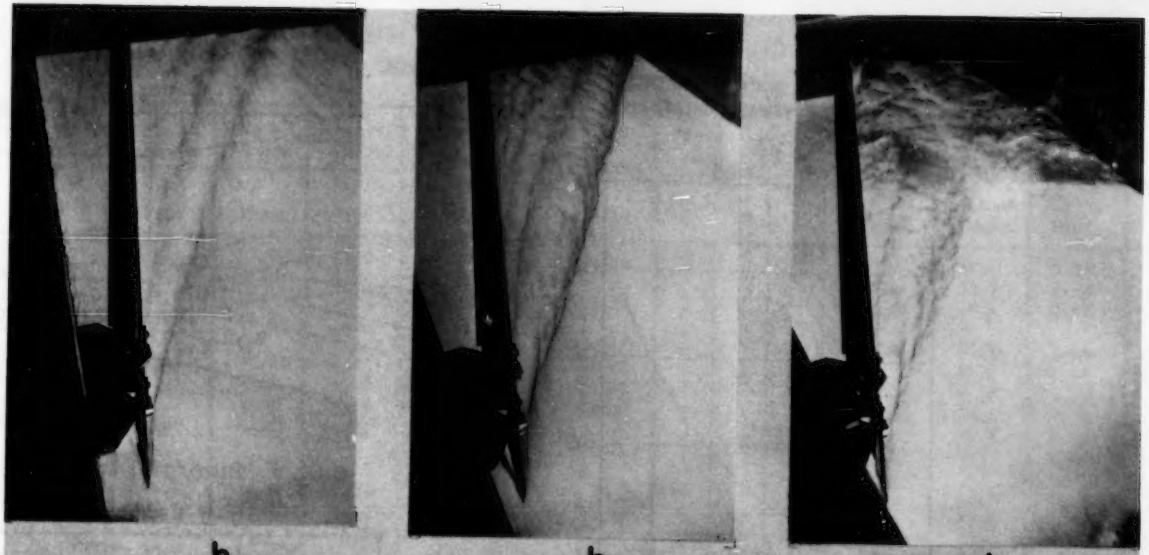

$\theta = 9°$ $\frac{h_2}{h_1} = 1.56$ UNDULAR

$\theta = 15°$ $\frac{h_2}{h_1} = 2.00$ ROLLER

$\theta = 21°$ $\frac{h_2}{h_1} = 2.45$ CHOKING

$F_1 = 3.20$

OBLIQUE HYDRAULIC JUMPS

FIG. 4

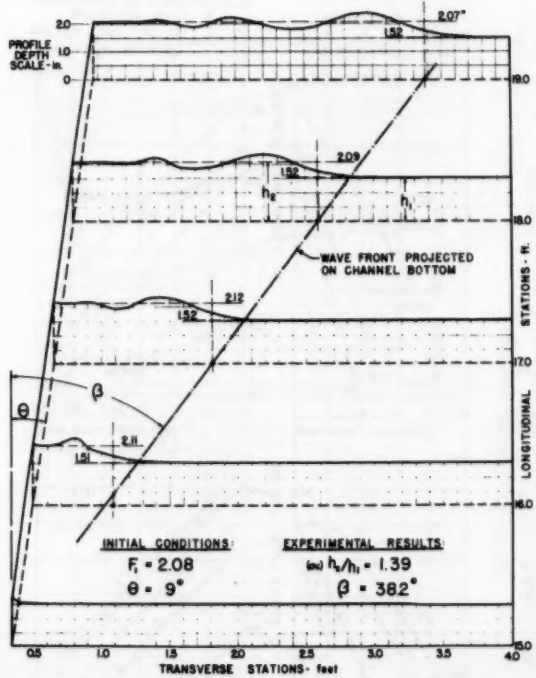

CROSS SECTIONS OF UNDULAR JUMP LOOKING DOWNSTREAM

FIG.5

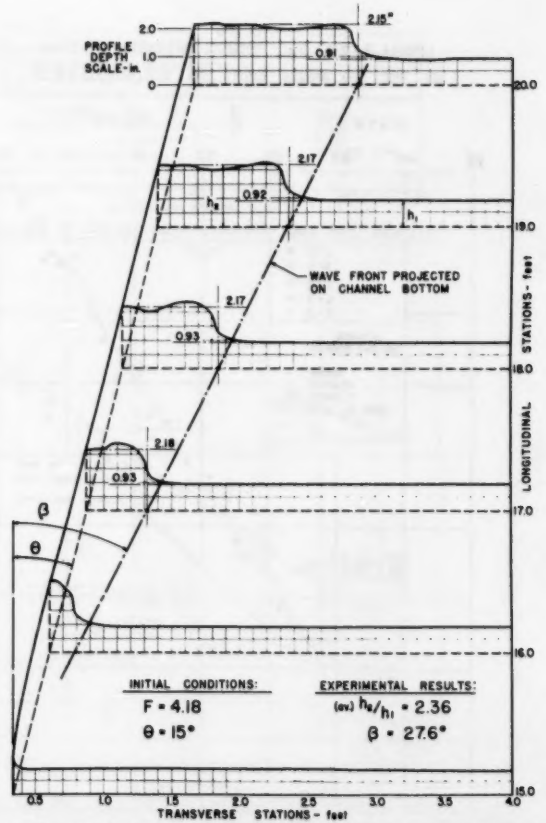

CROSS SECTIONS OF REGULAR JUMP LOOKING DOWNSTREAM

FIG.6

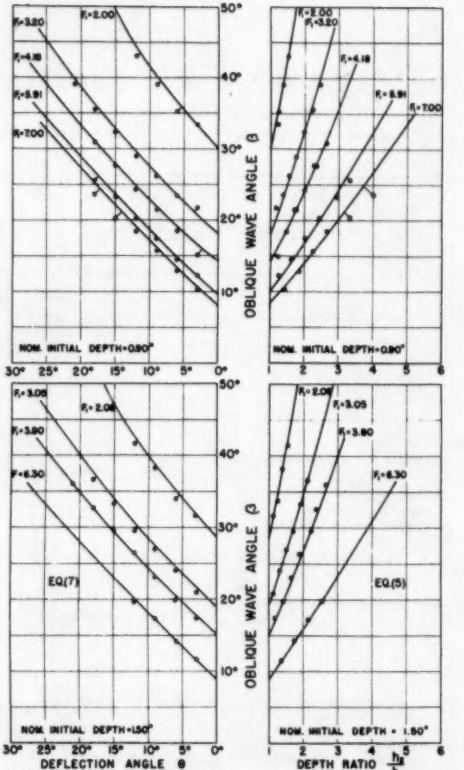

COMPARISON OF EXPERIMENTAL AND THEORETICAL VALUES FOR OBLIQUE JUMP ANGLES

COMPARISON OF EXP. AND THEOR. DEPTH RATIOS ACROSS AN OBLIQUE JUMP

FIG. 7

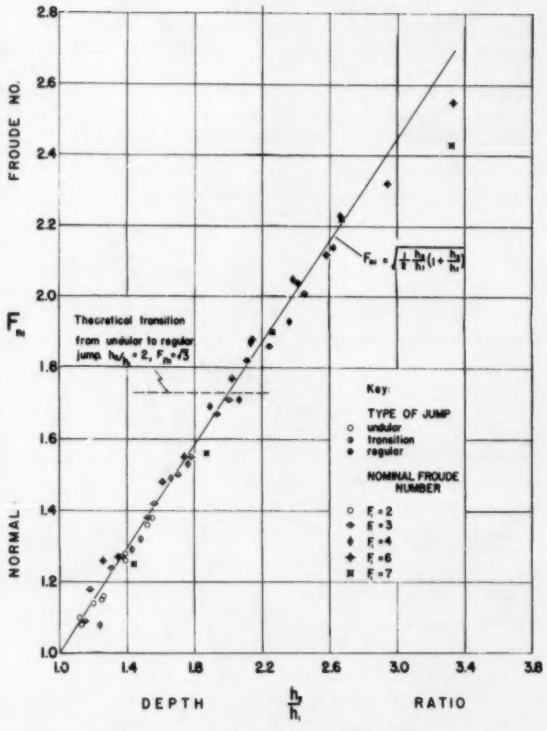

CLASSIFICATION OF JUMP FORM BY USE OF FROUDE NUMBER NORMAL TO WAVE FRONT

FIG. 8

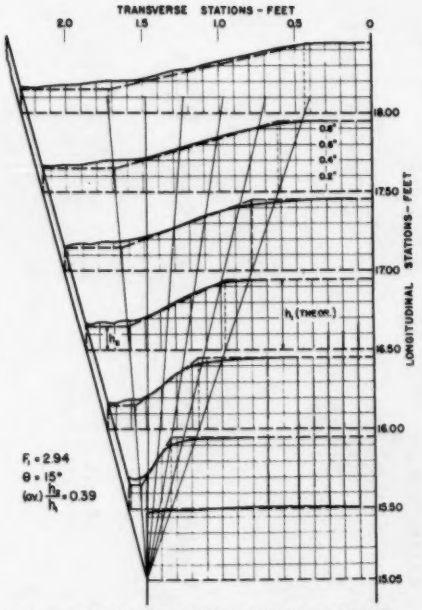

CROSS-SECTIONS OF FLOW IN EXPANSION ZONE

FIG. 9

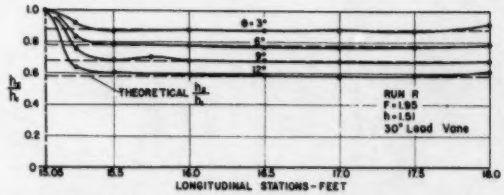

COMPARISON OF EXP AND THEOR. EXPANSION WAVE WALL PROFILES

FIG. 10

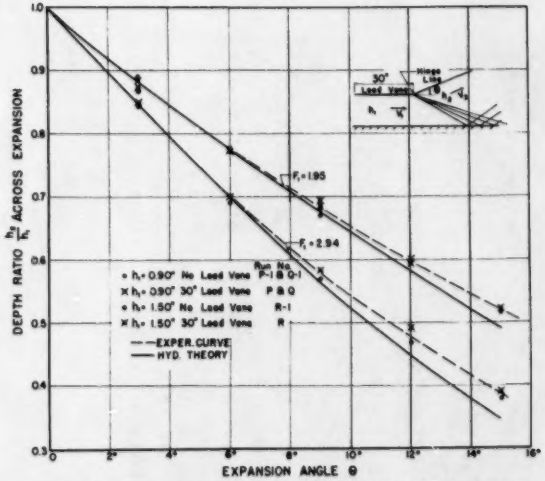
DEPTH RATIO $\frac{h_2}{h_1}$ ACROSS EXPANSION
EXPANSION ANGLE θ
30° Lead Vane
Hinge Line
$F_1 = 1.95$
$F_1 = 2.94$
Run No.
○ h_1 = 0.90" No Lead Vane P-1 & Q-1
× h_1 = 0.90" 30° Lead Vane P & Q
○ h_1 = 1.50" No Lead Vane R-1
× h_1 = 1.50" 30° Lead Vane R
EXPER. CURVE
HYD. THEORY

COMPARISON OF EXPERIMENTAL AND THEORETICAL DEPTH RATIOS ACROSS EXPANSION WAVES

FIG. 11

AMERICAN SOCIETY OF CIVIL ENGINEERS

OFFICERS FOR 1954

PRESIDENT

DANIEL VOIERS TERRELL

VICE-PRESIDENTS

Term expires October, 1954:
EDMUND FRIEDMAN
G. BROOKS EARNEST

Term expires October, 1955:
ENOCH R. NEEDLES
MASON G. LOCKWOOD

DIRECTORS

Term expires October, 1954:
WALTER D. BINGER
FRANK A. MARSTON
GEORGE W. McALPIN
JAMES A. HIGGS
I. C. STEELE
WARREN W. PARKS

Term expires October, 1955:
CHARLES B. MOLINEAUX
MERCEL J. SHELTON
A. A. K. BOOTH
CARL G. PAULSEN
LLOYD D. KNAPP
GLENN W. HOLCOMB
FRANCIS M. DAWSON

Term expires October, 1956:
WILLIAM S. LaLONDE, JR.
OLIVER W. HARTWELL
THOMAS C. SHEDD
SAMUEL B. MORRIS
ERNEST W. CARLTON
RAYMOND F. DAWSON

PAST-PRESIDENTS

Members of the Board

CARLTON S. PROCTOR
WALTER L. HUBER

EXECUTIVE SECRETARY
WILLIAM N. CAREY

TREASURER
CHARLES E. TROUT

ASSISTANT SECRETARY
E. L. CHANDLER

ASSISTANT TREASURER
GEORGE W. BURPEE

PROCEEDINGS OF THE SOCIETY

HAROLD T. LARSEN
Manager of Technical Publications

DEFOREST A. MATTESON, JR.
Editor of Technical Publications

PAUL A. PARISI
Assoc. Editor of Technical Publications

COMMITTEE ON PUBLICATIONS

FRANK A. MARSTON, *Chairman*

I. C. STEELE
ERNEST W. CARLTON
GLENN W. HOLCOMB
OLIVER W. HARTWELL
SAMUEL B. MORRIS